Inorganic Chemistry

Article

pubs.acs.org/IC

Gadolinium Sulfate Modified by Formate To Obtain Optimized Magneto-Caloric Effect

Long-Yang Xu,[†] Jiong-Peng Zhao,*[,†,§] Ting Liu,[†] and Fu-Chen Liu*[,†]

[†]School of Chemistry and Chemical Engineering, Tianjin University of Technology, No. 391 Binshui Xilu Road, Tianjin 300384, P. R. China

[§]School of Environmental and Energy Engineering, Beijing University of Technology, Beijing 100124, P. R. China

Supporting Information

ABSTRACT: Three new Gd^{III} based coordination polymers $[Gd_2(C_2H_6SO)(SO_4)_3(H_2O)_2]_n$ (**1**), $\{[Gd_4(HCOO)_2(SO_4)_5(H_2O)_6]\cdot H_2O\}_n$ (**2**), and $[Gd(HCOO)(SO_4)(H_2O)]_n$ (**3**) were obtained by modifying gadolinium sulfate. With the gradual increase of the volume ratio of HCOOH and DMSO in synthesis, the formate anions begin to coordinate with metal centers; this results in the coordination numbers of sulfate anion increasing and the contents of water and DMSO molecules decreasing in target complexes. Accordingly, spin densities both per mass and per volume were enhanced step by step, which are beneficial for the magneto-caloric effect (MCE). Magnetic studies reveal that with the more formate anions present, the larger the negative value of magnetic entropy change ($-\Delta S_m$) is. Complex **3** exhibits the largest $-\Delta S_m$ = 49.91 J kg^{-1} K^{-1} (189.51 mJ cm^{-3} K^{-1}) for T = 2 K and ΔH = 7 T among three new complexes.

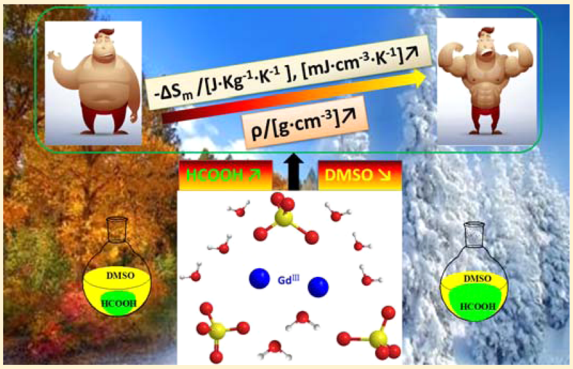

INTRODUCTION

Because of energy shortage and environmental impact issues, magnetic refrigeration, as an energy-efficient and environment friendly refrigeration technology, has been proposed as a good substitute for conventional compressor based refrigeration at low- and ultra-low-temperatures.[1] Since magnetic refrigeration relies on the magneto-caloric effect (MCE) illustrated by the change of the adiabatic temperature (ΔT_{ad}) and the isothermal magnetic entropy (ΔS_m) upon application or removal of the external magnetic field,[2,3] exploiting magnetic refrigerants with excellent MCE is particularly important.[4] Different kinds of materials have been studied for their MCE, especially the gadolinium based compounds, because the Gd^{III} ion has the largest spin ground state ($S = {}^7/_2$), which provides the largest entropy per single ion amounting to $R\ln(2S + 1)$, negligible magnetic anisotropy, and low-lying excited spin states.[1,5]

High-performing Gd^{III} based compounds in MCE should be high spin density or low M_W/N_{Gd} (M_w = molecular weight, N_{Gd} = number of Gd^{3+} ions).[5,6] To achieve this goal, complexes varying from discrete molecules to high-dimensional frameworks were reported on the basis of different kinds of ligands. To date, some Gd^{III} based compounds with OH^-, CO_3^{2-}, $C_2O_2^{2-}$, $CH_3CO_2^{2-}$, and HCO_2^- as ligands were reported taking on impressive MCE.[5,7−9] The representative complex, $[Gd(OH)CO_3]_n$ reported by Tong et al., exhibits the highest MCE.[7c] From the complexes reported, it can be found that ligands with low molecular weight, multinegative charge, and high coordination number contribute to high magnetic density. For this, the sulfate anion rightly satisfies these requests; however, there are a few examples of MCE about gadolinium based compounds bridged by sulfate anion. For example, $Gd_2(SO_4)_3\cdot 8H_2O$ as a simple paramagnetic salt became an interesting subject of the very first adiabatic demagnetization experiments and the attainment of temperature below 1 K.[10] Very recently, Bu et al. reported two polymers based on $[Gd_4(OH)_4]^{8+}$ units bridged by sulfate with or without cobridged $C_2O_2^{2-}$.[11] In these results, weak exchange interactions and relatively high density of metal sulfate lead to considerable MCE.[10,11] Therefore, modifying gadolinium sulfate with other small ligands will achieve high spin density with large MCE.

On the basis of the strategy mentioned above, the smallest organic carboxylate, formate, was selected as coligand to modify gadolinium sulfate. Fortunately, three complexes $[Gd_2(C_2H_6SO)(SO_4)_3(H_2O)_2]_n$ (**1**), $\{[Gd_4(HCOO)_2(SO_4)_5(H_2O)_6]\cdot H_2O\}_n$ (**2**) and $[Gd(HCOO)(SO_4)(H_2O)]_n$ (**3**) were obtained step by step via hydrothermal reaction of $Gd_2(SO_4)_3\cdot 8H_2O$ and HCOOH in DMSO. As the amount of formic acid increases in the synthesis, formate anions begin to coordinate with metal centers, coordination numbers of sulfate anion are increasing, and most of the solvent molecules coordinated with Gd^{III} ions are excluded. Accordingly, low M_W/N_{Gd} and high density are obtained step by step. Magnetic studies reveal that

Received: January 28, 2015
Published: May 15, 2015

DOI: 10.1021/acs.inorgchem.5b00214
Inorg. Chem. 2015, 54, 5249−5256

the more formate anions present, the larger $-\Delta S_m$ is, and **3** exhibits the largest $-\Delta S_m$ = 49.91J kg^{-1} K^{-1} (189.51 mJ cm^{-3} K^{-1}) at T = 2 K and ΔH = 7 T.

EXPERIMENTAL SECTION

Materials and Physical Measurements. All the reagents for synthesis were obtained commercially and used as received. The FT-IR spectra were recorded from KBr pellets in the range 4000−400 cm^{-1} on a TENSOR 27 (Bruker) spectrometer. The X-ray powder diffraction (XRPD) was recorded on a Rigaku D/Max-2500 diffractometer at 60 kV, 300 mA for a Cu-target tube and a graphite monochromator. Thermogravimetric analysis (TGA) was carried out on a standard TGA−DTA analyzer under a nitrogen flow at a heating rate of 2 °C min^{-1} for all measurements. Simulation of the XRPD spectra was carried out by the single-crystal data and diffraction-crystal module of the Mercury (Hg) program available free of charge via the Internet at http://www.iucr.org. Magnetic data were collected on crushed crystals of the sample on a Quantum Design MPMS XL-7 SQUID magnetometer.

Synthesis of $[Gd_2(C_2H_6SO)(SO_4)_3(H_2O)_2]_n$ ***(1)***. Complex **1** was obtained by the following hydrothermal method: A mixture of $Gd_2(SO_4)_3{\cdot}8H_2O$ (4 mmol), HCOOH (2 mL), and DMSO (6 mL) was sealed in a Teflon-lined autoclave and heated to 140 °C over 6 h. After the reaction vessel was maintained for 48 h, it was cooled to room temperature over 18 h. Colorless block crystals of **1** were harvested with ca. 40% yield based on Gd. FT-IR (KBr pellet, cm^{-1}): 3185, 1650, 1401, 1125, 605.

Synthesis of $\{[Gd_4(HCOO)_2(SO_4)_5(H_2O)_6]{\cdot}H_2O\}_n$ ***(2)***. Single crystals of **2** suitable for X-ray analysis were obtained by the following hydrothermal method: A mixture of $Gd_2(SO_4)_3{\cdot}8H_2O$ (4 mmol), HCOOH (3 mL), and DMSO (5 mL) was sealed in a Teflon-lined autoclave and heated to 140 °C over 6 h. After the reaction vessel was maintained for 48 h, it was cooled to room temperature over 18 h, and colorless needlelike crystals of **2** were harvested with ca. 25% yield based on Gd. FT-IR (KBr pellet, cm^{-1}): 3385, 1572, 1400, 1136, 606.

Synthesis of $[Gd(HCOO)(SO_4)(H_2O)]_n$ ***(3)***. Complex **3** was obtained by the following hydrothermal method: A mixture of $Gd_2(SO_4)_3{\cdot}8H_2O$ (4 mmol), HCOOH (4 mL), and DMSO (4 mL) was sealed in a Teflon-lined autoclave and heated to 140 °C over 6 h. After the reaction vessel was maintained for 48 h, it was cooled to room temperature over 18 h. Colorless cone-shaped crystals of **3** were harvested with ca. 35% yield based on Gd. FT-IR (KBr pellet, cm^{-1}): 3366, 1565, 1379, 1347, 1151, 1035, 806, 602.

X-ray Data Collection and Structure Determinations. X-ray single-crystal diffraction data for complexes **1**−**3** were collected on a Rigaku SCXmini diffractometer at 293(2) K with Mo Kα radiation (λ = 0.710 73 Å) by ω scan mode. The program Rigaku CrystalClear[12a] was used for integration of the diffraction profiles. All the structures were solved by direct methods using the SHELXS program of the SHELXTL package and refined by full-matrix least-squares methods with SHELXL.[12b] Final refinement was performed by full matrix least-squares methods with anisotropic thermal parameters for non-hydrogen atoms on F^2. CCDC 1012085−1012087 contain the supplementary crystallographic data for this paper. These data can be obtained free of charge from The Cambridge Crystallographic Data Centre via www.ccdc.cam.ac.uk/data_request/cif. Details of the X-ray crystal structure analysis of **1**, **2**, and **3** are summarized in Table 1.

RESULTS AND DISCUSSION

Description of Complexes 1−3. $[Gd_2(SO_4)_3(C_2H_6SO)(H_2O)_2]_n$ ***(1)***. Complex **1** crystallizes in the monoclinic space group $P2_1/c$. The asymmetric unit of **1** contains two Gd^{III} ions, three sulfate anions, two water molecules, and one DMSO molecule. The Gd1 ion is coordinated by eight O atoms from five sulfate anions, one water molecule, and one DMSO, while the Gd2 ion is coordinated by seven O atoms from six sulfate anions and one water molecule (Figure 1a). The range of Gd−O bond lengths is 2.289(8)−2.595(7) Å. Three sulfate anions

Table 1. Crystal Data and Structure Refinement for 1−3

	1	2	3
chemical formula	$C_2H_{10}Gd_2O_{15}S_4$	$C_2H_{14}Gd_4O_{30}S_5$	CH_3GdO_7S
fw	716.80	1323.48	316.34
cryst syst	monoclinic	monoclinic	tetragonal
space group	$P2_1/c$	$C2/c$	$P4_1$
a (Å)	9.1707(18)	19.439(4)	6.9095(10)
b (Å)	17.328(3)	12.991(5)	6.9095(10)
c (Å)	9.7449(19)	9.7163(19)	11.591(2)
β/deg	111.77(3)	93.31(3)	90.00
V/Å^3	1438.1(6)	2449.5(12)	553.37(19)
Z	4	4	4
D (g cm^{-3})	3.311	3.589	3.797
μ (mm^{-1})	9.801	11.251	12.34
F (000)	1296.0	2440.0	580.0
reflns collected	12 308	12 669	4829
indep reflns	2529	2789	969
obsd reflns	2427	2596	965
R_{int}	0.083	0.070	0.043
GOF	1.044	1.101	1.066
T/K	293(2)	293(2)	293(2)
R1^a/wR2^b	0.0528/0.1274	0.0301/0.0726	0.0250/0.0597

$^aR = \sum||F_o| - |F_c||/\sum|F_o|$. $^bR_w = [\sum[w(F_o^2 - F_c^2)^2]/\sum w(F_o^2)^2]^{1/2}$.

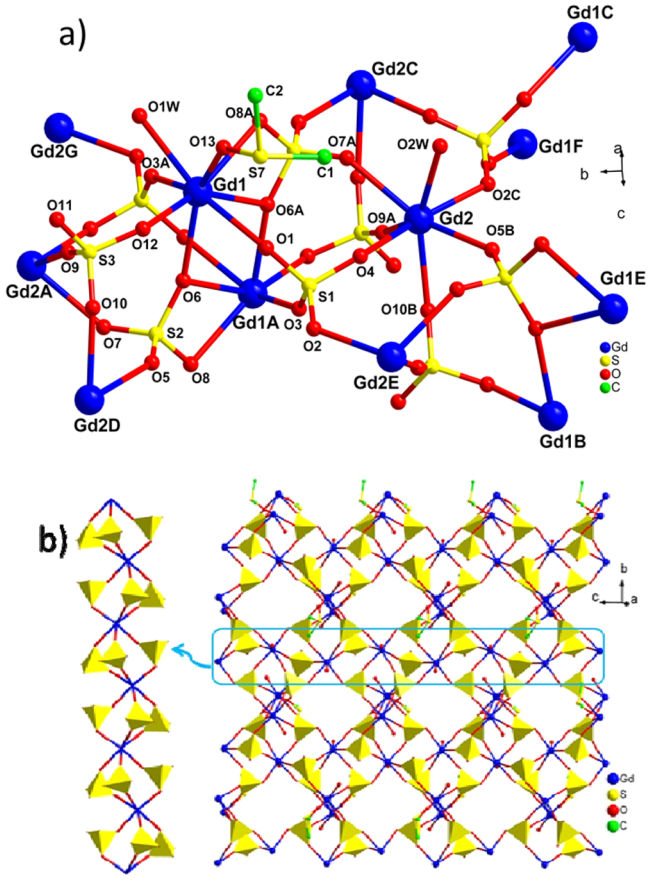

Figure 1. (a) Coordination environment and linkage modes of sulfate anions, DMSO, and Gd^{III} ions in **1** (all H atoms omitted for clarity). Symmetry codes: (A) $-x+1, -y+2, -z$; (B) $-x+1, y-{}^1/_2, -z+{}^1/_2$; (C) $x, -y+{}^3/_2, z-{}^1/_2$; (D) $-x+1, y+{}^1/_2, -z+{}^1/_2$; (E) $x, -y+{}^3/_2, z+{}^1/_2$; (F) $1-x, -{}^1/_2+y, -{}^1/_2-z$; (G) $1-x, {}^1/_2+y, -{}^1/_2-z$. (b) Polyhedron views of the 2D structure as well as the particular 1D chain of complex **1**.

DOI: 10.1021/acs.inorgchem.5b00214
Inorg. Chem. 2015, 54, 5249−5256

take different coordinated modes. The first one takes μ_4-η^1 mode coordinated to Gd1, Gd2E, Gd1A, and Gd2 ions by O1, O2, O3, and O4. The second one bridges Gd1A, Gd2D, Gd1, and Gd2A ions in the μ_4-η^1:η^2 bridging mode. The last one acts as a tridentate ligand, and links Gd1, Gd2D, and Gd2A with the μ_3-η^1 mode. Selected bond lengths of **1** are given in Supporting Information Table S1. In complex **1**, O6 and O6A bridging Gd1 and Gd1A give a dimer, while Gd2 ions and sulfate anions give a particular 1D chain (Figure 1b). These 1D chains are connected by the dimers via sulfate anions to form the 2D structure (Figure 1b).

*{[Gd$_4$(HCOO)$_2$(SO$_4$)$_5$(H$_2$O)$_6$]·H$_2$O}$_n$ (**2**).* Complex **2** crystallizes in the monoclinic space group *C*2/*c*. The asymmetric unit of **2** contains two Gd^{III} ions, a formate anion, two and a half sulfate anions, three coordinated water molecules, and half a lattice water molecule. As shown in Figure 2, the Gd1 ion possesses a distorted GdO_9 coordination environment coordinated by five sulfate anions, two formate anions, and one water molecule. The Gd2 ion takes a distorted GdO_8 square antiprism, coordinated by five sulfate anions, one formate anion, and two water molecules. Three sulfate anions taking the μ_4-η^1 mode coordinate to four different Gd^{III} ions by four oxygen atoms. In complex **2**, the formate anion adopts the μ_3-η^2 coordination mode coordinated to Gd1, Gd2I, and Gd1A ions by O11 and O12. The range of Gd−O bond lengths is 2.306(4)−2.595(4) Å (Supporting Information Table S1). There is a particular Gd4 cluster linked by two formate anions (Figure 2). These Gd4 clusters are connected by the tetradentate sulfate anions to form a 2D layer (Figure 3a). Furthermore, these 2D layers are connected by tetradentate sulfate anions along the *a* axis, forming a beautiful reticular structure presented in Figure 3b with lattice water filing in the channels. Compared with **1**, the coordinated number of sulfate anions increases, and the DMSO molecules are crowded out by formate anions.

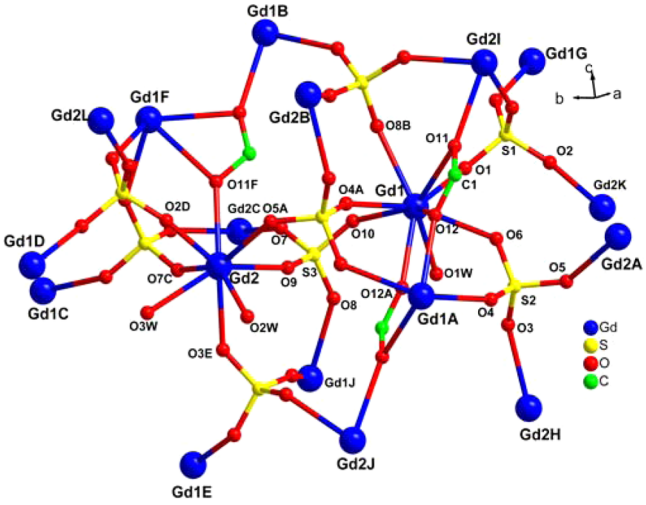

Figure 2. Coordination environment and linkage modes of sulfate anions, formate anions and Gd^{III} ions in **2** (all H atoms omitted for clarity). Symmetry codes: (A) $-x+{}^1/_2, -y+{}^1/_2, -z$; (B) $x, -y+1, z+{}^1/_2$; (C) $-x+{}^1/_2, -y+{}^3/_2, -z$; (D) $x-{}^1/_2, y+{}^1/_2, z$; (E) $-x+{}^1/_2, y+{}^1/_2, -z-{}^1/_2$; (F) $-x+{}^1/_2, y+{}^1/_2, -z+{}^1/_2$; (G) $-x+1, y, -z+{}^1/_2$; (H) $-x+{}^1/_2, y-{}^1/_2, -z-{}^1/_2$; (I) $-x+{}^1/_2, y-{}^1/_2, -z+{}^1/_2$; (J) $x, -y+1, z-{}^1/_2$; (K) $x+{}^1/_2, y-{}^1/_2, z$; (L) $-x, y, {}^1/_2-z$.

*[Gd(HCOO)(SO$_4$)(H$_2$O)]$_n$ (**3**).* Complex **3** crystallizes in the tetragonal $P4_1$ space group, and the asymmetric unit of **3** contains a Gd^{III} ion, a formate anion, a sulfate anion, and one water molecule (Figure 4). As shown in Figure 4, the Gd^{III} ion is present in a distorted GdO_9 polyhedron, coordinated by three formate anions, four sulfate anions, and one water molecule. The range of Gd−O bond lengths is 2.319(9)−2.675(11) Å (Supporting Information Table S1). The sulfate anions coordinate to four different Gd^{III} ions with four oxygen atoms. In complex **3**, the formate anions adopt a μ_3-η^2 mode that bridges Gd1, Gd1E, and Gd1H. As shown in Figure 5a, Gd^{III} ions are bonded by bridging O atoms from formate anions to construct a helical chain. Neighboring helical chains with the same chirality are connected by formate anions to form a chiral metal formate framework. The tetradentate sulfate anions also linked the gadolinium to construct a 3D net, which enhances the metal framework (Figure 5b). Compared with **2**, only one coordinated water molecule was left.

From the description above, the structure of **3** has two parts: one is the gadolinium−formate framework, and the other is the gadolinium−sulfate framework. It is interesting that formate anions and Gd^{III} ions in the 3D formate−gadolinium structure can be considered to be 3-connected nodes and give a (10^3)-b (*ths*) topology net (Supporting Information Figure S3). Similarly, if sulfates and Gd^{III} ions in sulfate−gadolinium structure are treated as 4-connected node, a $(4^2.8^4)$ (*uoc*) topology net is constructed by sulfate anions and gadolinium

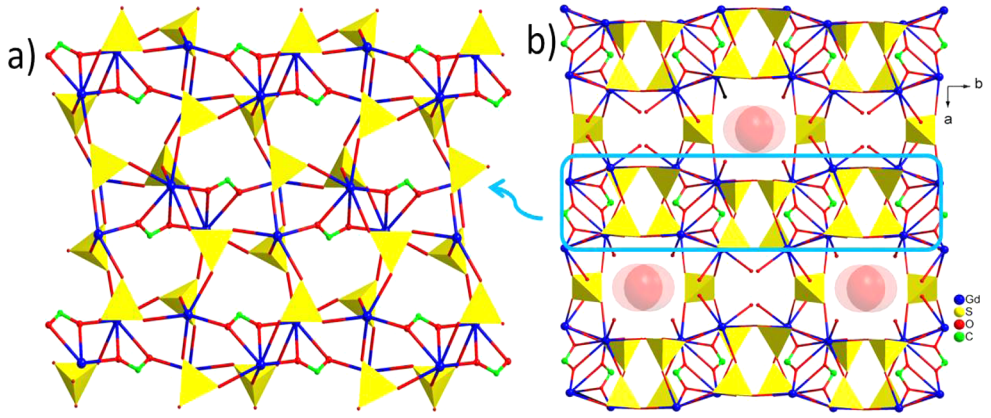

Figure 3. (a) 2D layer assembled by Gd4 clusters and sulfates of **2** (water molecules and H atoms are removed for clarity). (b) Polyhedron view of the 3D structure of **2** along the *c* axis.

DOI: 10.1021/acs.inorgchem.5b00214
Inorg. Chem. 2015, 54, 5249−5256

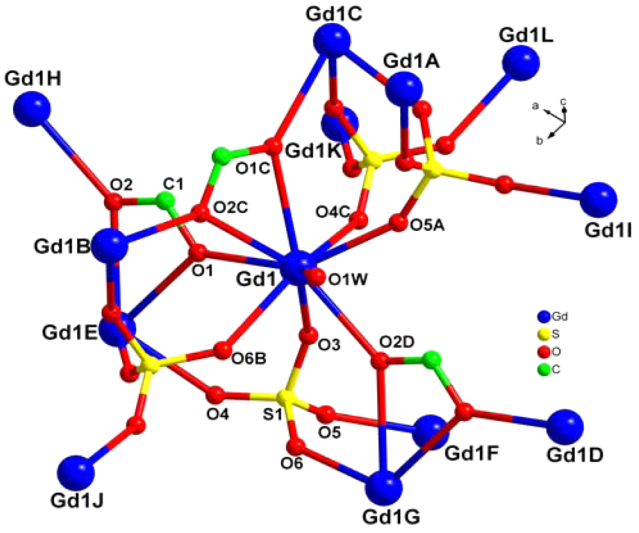

Figure 4. Coordination environment and linkage modes of sulfate anions, formate anions, and Gd^{III} ions in **3** (all H atoms omitted for clarity). Symmetry codes: (A) $-x, -y + 1, z + {}^1/_2$; (B) $-y + 1, x + 1, z + {}^1/_4$; (C) $-y + 1, x, z + {}^1/_4$; (D) $x - 1, y, z$; (E) $y, -x + 1, z - {}^1/_4$; (F) $-x, -y + 1, z - {}^1/_2$; (G) $y - 1, -x + 1, z - {}^1/_4$; (H) $x + 1, y, z$; (I) $-y, x, z + {}^1/_4$; (J) $x, 1 + y, z$; (K) $y, -x, z - {}^1/_4$; (L) $x, -y + 1, z$.

ions (Supporting Information Figure S4). When the whole framework is considered, formate anions, sulfate anions, and Gd^{III} ions can be considered as the 3-, 4-, and 7-connected nodes, respectively. Then, the whole framework could be simplified as a 3-nodal (3, 4, 7)-connected network with the Schläfli symbol of $(4^2.6)$ $(4^3.6^3)$ $(4^8.6^{10}.8^3)$ (Figure 6).[13]

Herein, we need to further summarize the process of obtaining three new Gd^{III} based coordination polymers bridged by sulfate. As is shown in Figure 7, the design and synthesis of three new Gd^{III} based coordination polymers is realized step-by-step. In **1**, the water and DMSO molecules coordinate to Gd^{III} centers as terminal groups with the M_W/N_{Gd} of **1** being 358.4, so the extension of the 2D network is impossible. When the volume ratio of HCOOH and DMSO was augmented, complex **2** was obtained in which the number of coordination water molecules is decreased and DMSO molecules are crowded out by formate anions. Subsequently, complex **2** extends itself into the 3D framework with the M_W/N_{Gd} of **2** of 330.9, which is smaller than that of **1**. However, complex **2** is not the end, because there are still too many water molecules, which are not good for MCE. With the hope of obtaining

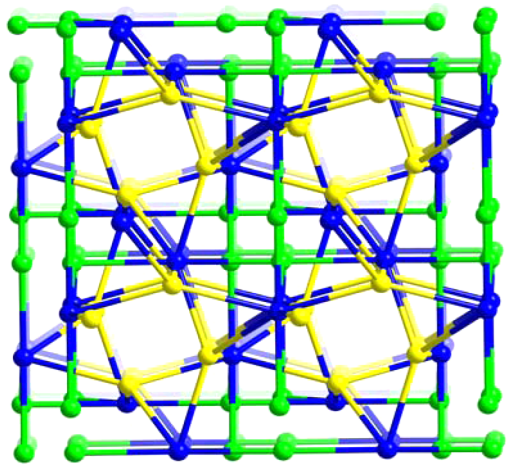

Figure 6. Schematic view of the (3, 4, 7)-connected network topology of **3**. Gd atoms are shown as blue, the yellow spheres represent sulfate anions, and bright green spheres represent formate anions.

considerable M_W/N_{Gd}, the volume ratio of HCOOH and DMSO continues to be augmented. As expected, most of the water molecules are crowded out by formate anions, which result in the smallest M_W/N_{Gd} with a value of 316.3 among the three complexes. When augmenting the volume ratio of HCOOH and DMSO further, there are not any complexes obtained. From the sketch map, it is clear to find that the more formate present in raw material, the lower M_W/N_{Gd} is. In complex **1**, water and DMSO molecules coordinate with Gd^{III}, which is not good for low M_W/N_{Gd}. In complex **2**, the DMSO molecules are crowded out by formate anions, which is beneficial to lower M_W/N_{Gd}. In complex **3**, not only the DMSO molecules but also most water molecules are crowded out by formate anions, which gives the lowest M_W/N_{Gd} among these three polymers.

Magnetic Studies. Magnetic susceptibility data was collected for crystalline samples of **1**−**3**, and the phase purity of these samples was confirmed by XRPD in Supporting Information Figure S1. Also, TGA results indicate **1** and **3** are stable until about 280 °C, while complex **2** begin losing the lattice and coordinated water molecules at about 110 °C, see Supporting Information Figure S2. The data for **1** collected in the 2−300 K temperature range under external field 1 kOe is shown in Figure 8a corresponding to one Gd^{III} ion. As the temperature decreases, the $\chi_M T$ values stay almost constant at

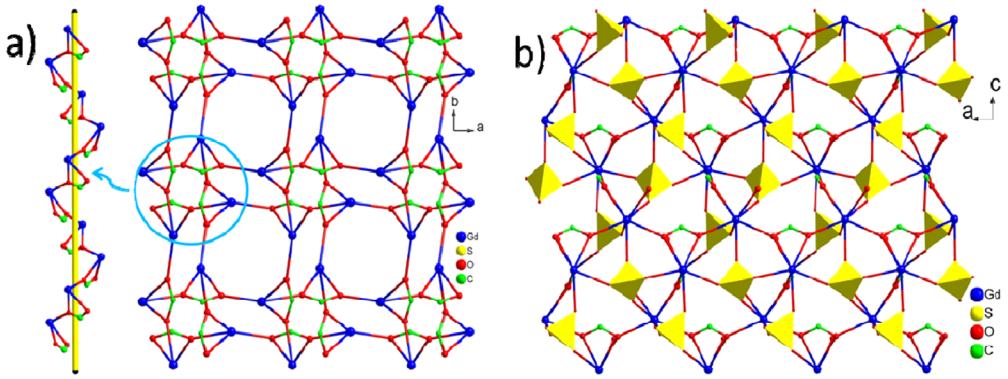

Figure 5. (a) Chiral framework of **3** and the helical chain in **3** (sulfate anions and water molecules are removed for clarity). (b) Polyhedron view of the 3D structure of **3**.

DOI: 10.1021/acs.inorgchem.5b00214
Inorg. Chem. 2015, 54, 5249−5256

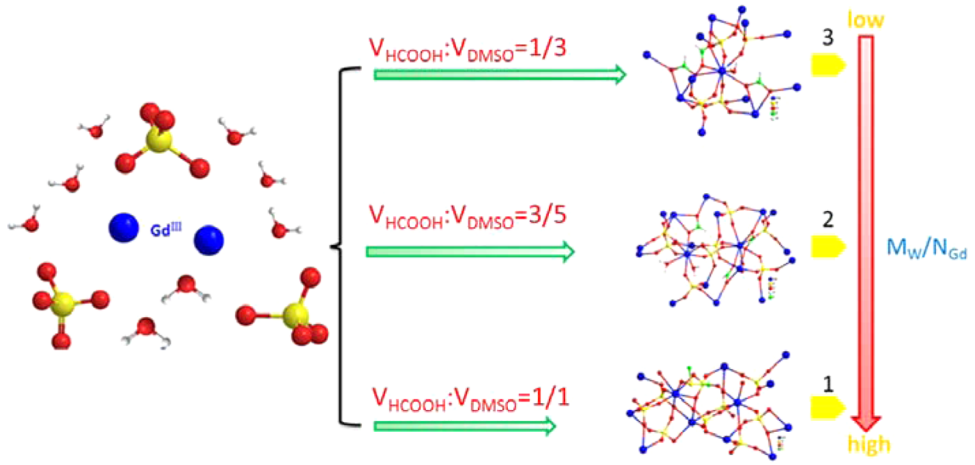

Figure 7. Sketch map of design and synthesis of three new Gd^{III} based coordination polymers.

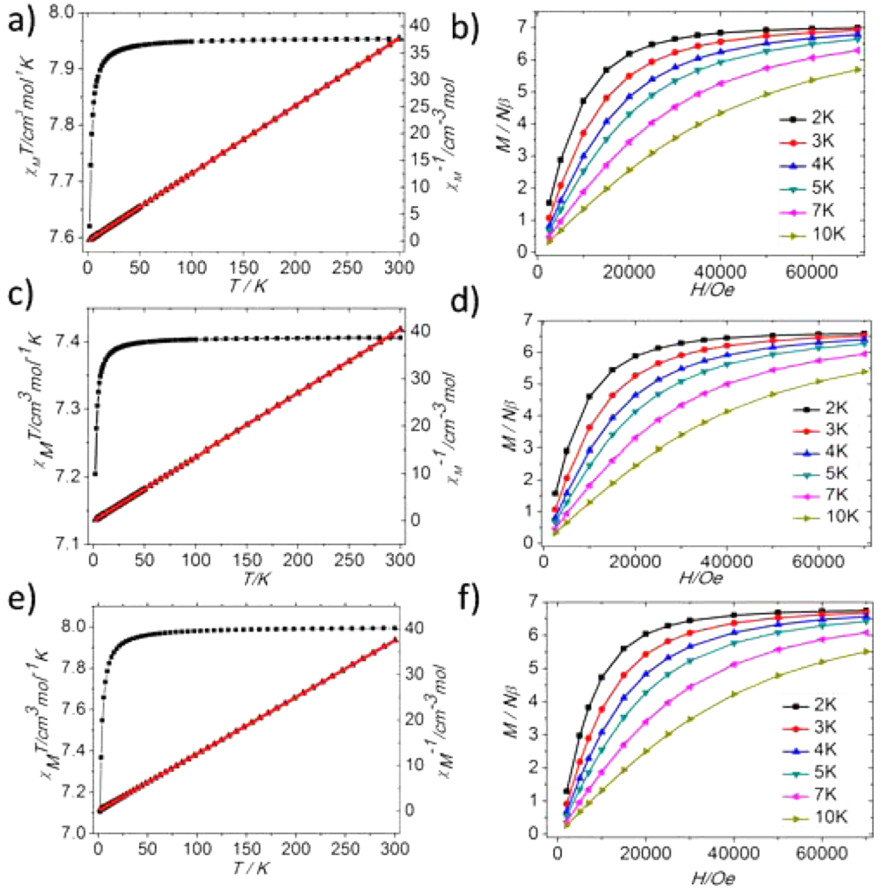

Figure 8. Thermal variation of $\chi_M T$ vs T, $1/\chi_M$ vs T plots, and magnetization data in applied different fields between 2 and 10 K: (a, b) **1**, (c, d) **2**, (e, f) **3**.

high temperatures and decrease sharply below 25 K. The data follows the Curie–Weiss law ($\chi_M = C/(T - \theta)$), giving the best fitted parameters $C = 7.95$ cm^3 K mol^{-1}, $\theta = -0.09$ K for **1**. The C value is consistent with the expected value of one magnetically isolated Gd^{III} ion ($S = {}^7/_2$, $g = 2.0$). Also, the very small negative Weiss constants may be related to complex magnetic correlations, which are very weak anyhow.

The field-dependent magnetizations of **1** at different temperature between 2 and 10 K are shown in Figures 8b and 9a. The shapes of the magnetization of **1** also suggested weak magnetic interactions between the adjacent metal ions. Also, as shown in Figure 9a, the magnetization at different temperatures appears almost as a superposition suggesting that **1** is an isotropic complex. The weak magnetic interactions and large metal/ligand mass ratio make **1** a promising candidate for low-temperature magnetic cooling, as magnetic entropy change ΔS_m, a key parameter in evaluating the MCE, can be derived from the Maxwell relations by integrating over the magnetic field change, $\Delta S_m(T)_{\Delta H} = \int [\partial M(T, H)/\partial T]_H \, dH$.[14] The entropy changes at various magnetic fields and temperatures are

DOI: 10.1021/acs.inorgchem.5b00214
Inorg. Chem. 2015, 54, 5249–5256

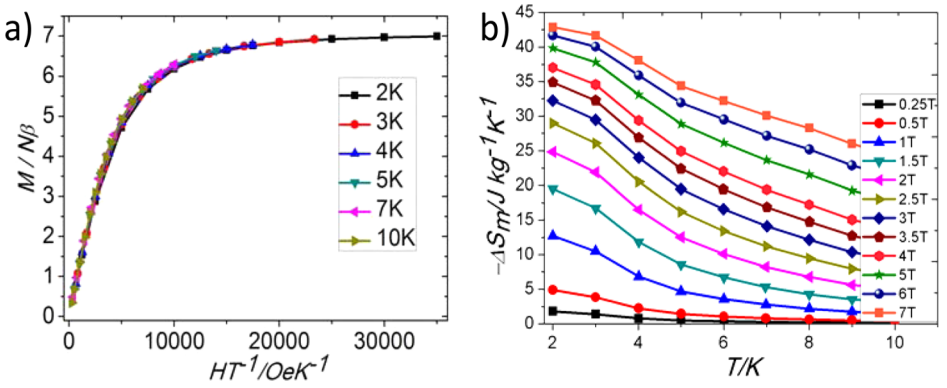

Figure 9. (a) M vs HT^{-1} data in applied different fields between 2 and 10 K, for complex **1**; (b) experimental $-\Delta S_m$ obtained from the magnetization data of **1** at various fields and temperatures.

summarized in Figure 9b, with an impressive value of 42.88 J kg^{-1} K^{-1} for T = 2 K and ΔH = 7 T. The $-\Delta S_m$ of **1** is smaller than the theoretical value of 48.24 J kg^{-1} K^{-1} for one uncoupled Gd^{III} ion (judged by $2R\ln(2S+1)$, where R is the gas constant and S is the spin state). The gap between the experimental data and the theoretical value may originate from the antiferromagnetic interactions in **1**.

The magnetic susceptibility data that of **2** and **3** was collected in the 2−300 K temperature range under external field 1 kOe as shown in Figure 8c,e corresponding to one Gd^{III} ion, respectively. For **2** and **3**, as the temperature decreases, the $\chi_M T$ values stay almost constant at high temperatures and decrease sharply below 25 K, suggesting weak antiferromagnetic (AF) coupling between the Gd^{III} ions. The data follows the Curie−Weiss law ($\chi_M = C/(T-\theta)$), giving the best fitted parameters, C = 7.40 cm^3 K mol^{-1}, θ = −0.056 K for **2**, and C = 8.00 cm^3 K mol^{-1}, θ = −0.25 K for **3** (Figure 8c,e). The C values are consistent with the expected values of one magnetically isolated Gd^{III} ion ($S = {}^7/_2$, g = 2.0). Also, the very small negative Weiss constants may be related to weak magnetic interactions between the metal ions.

The field-dependent magnetizations of **2** and **3** at different temperatures between 2 and 10 K are shown in Figure 8d,f. Like that of **1**, the shapes of the magnetization also suggested weak magnetic interactions between the adjacent metal ions in **2** and **3**. Also, as shown in Figures 10a and 11a, the M versus HT^{-1} plots at different temperatures appear as almost a superposition suggesting that **2** and **3** are isotropic polymers. Compared with the M_W/N_{Gd} = 358.4 in **1**, the value of M_W/N_{Gd} in **2** and **3** is smaller (330.87 for **2** and 316.3 for **3**). The weak magnetic interactions and large metal/ligand mass ratios make **2** and **3** promising candidates for low-temperature magnetic cooling. The magnetic entropy changes of **2** at various magnetic fields and temperatures are summarized in Figure 10b, with an impressive of 43.40 J kg^{-1} K^{-1} for T = 2 K and ΔH = 7 T. The value of **2** is smaller than the theoretical value of 52.25 J kg^{-1} K^{-1} for one uncoupled Gd^{III} ion. The magnetic entropy changes of **3** at various magnetic fields and temperatures are summarized in Figure 11b, with an impressive of 49.91 J kg^{-1} K^{-1} for T = 2K and ΔH = 7 T, which is smaller than the theoretical value about 54.71 J kg^{-1} K^{-1} of **3**.

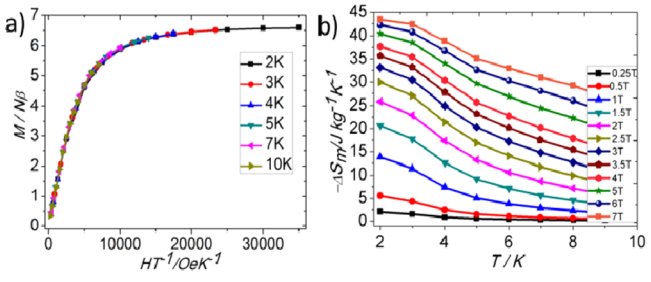

Figure 10. (a) M vs HT^{-1} data in applied different fields between **2** K and 10 K, for complex **2**; (b) Experimental $-\Delta S_m$ obtained from the magnetization data of **2** at various fields and temperatures.

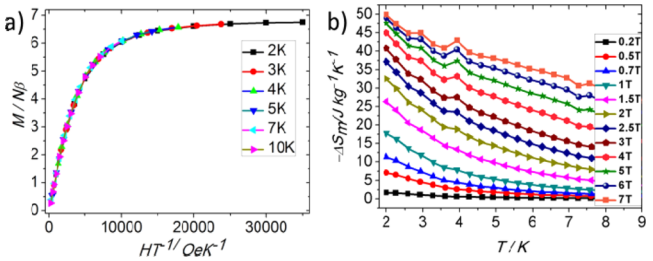

Figure 11. (a) M vs HT^{-1} data in applied different fields between 2 and 10 K, for complex **3**. (b) Experimental $-\Delta S_m$ obtained from the magnetization data of **3** at various fields and temperatures.

With the decrease of the mass of the complexes per one Gd^{III} ion in **1**−**3**, the maximum theoretical value for entropy change is increased. The maximum experimental value of the entropy change has the same tendency, but all the maximum experimental values do not reach the theoretical value, especially that for **2**. That may be due to the complex magnetic interactions between the metal ions in **2**, despite the excellent studies about the relationship between exchange coupling and the magneto-caloric effect.[15] However, it is hard to evaluate the relationship between magnetic interactions and MCE, due to the high dimensionality and low symmetry of complexes **1**−**3**. For the same reason, the accurate value of coupling constants cannot be obtained, so there is only a brief discussion about the effect of magnetic coupling on the entropy changes. Compared with the interactions conducted by the sulfate anions, the magnetic coupling conducted by the μ_{-2}-O bridges of the formate may be much more important for **2** and **3**. In **2** there are primarily two magnetic exchange pathways conducted by formate: double μ_{-2}-O bridges O12 and O12A link Gd1 and Gd1A with a bond angle Gd1−O12−Gd1A of 114.7° and Gd1···Gd1A distances of about 4.2 Å; single μ_{-2}-O bridge O11 links Gd1 and Gd2I with bond angle Gd1−O11−Gd2I of 134.2° and Gd1···Gd2I distances of about 4.6 Å. From the density functional calculations, it is proposed that the maximum

DOI: 10.1021/acs.inorgchem.5b00214
Inorg. Chem. 2015, 54, 5249−5256

ferromagnetic interactions are present with a Gd−O−Gd angle of 120°, and increasing or decreasing the angle from this point enhances the antiferromagnetic contribution.[15c] Thus, a weak ferromagnetic interaction is conducted by the double μ_{-2}-O bridges. The connected detail of the doubly μ_{-2}-O bridged Gd_2 dimer is very like that in the $[\{Gd(OAc)_3(H_2O)_2\}_2]\cdot 4H_2O$, in which obtained maximum entropy changes were close to the theoretical value for the weak ferromagnetic interactions conducted by the H-bonds between the dimers, which enhance the $-\Delta S_m$.[5a,15c] However, in **2** the Gd1 dimer is antiferromagnetically coupled with two Gd2 ions, which reduce the $-\Delta S_m$ greatly and lead to obvious difference between theoretical and experiment values, while in **3**, the Gd^{III} ions bridged by the μ_{-2}-O with Gd−O−Gd2 angles are about 135−138° but with long Gd···O distances (2.5−2.7 Å) and Gd···Gd distances (4.7−4.9 Å). Those long distances favor very weak magnetic interactions; for this, the obtained largest entropy change is much close to the theoretical value.

Among reported molecule based magnetic cryogens, magnetic entropy changes above 40.0 J kg^{-1} K^{-1} are limited, as listed in Table 2.[16−22] Magnetic entropy changes of the three new style molecule based magnetic cryogens are all above 40.0 J kg^{-1} K^{-1}. Also, it is more competitive when considered from the volumetric aspect: 141.98 mJ cm^{-3} K^{-1} for **1**, 155.76 mJ cm^{-3} K^{-1} for **2**, 189.51 mJ cm^{-3} K^{-1} for **3** (Table 2). Magnetic studies reveal that the more formate ions present, the larger MCE is. Complex **3** exhibits the largest $-\Delta S_m$ with 49.91J kg^{-1} K^{-1} (189.51 mJ cm^{-3} K^{-1}) for T = 2 K and ΔH = 7 T among three complexes. Indeed, evaluating molecule based magnetocaloric materials from a volumetric aspect is meaningful for practical application.[23] The $-\Delta S_m$ value of complex **3** is close to the value of two complexes $[Gd_4(SO_4)_4(\mu_3\text{-}OH)_4(H_2O)_n]_n$ and $[Gd_4(\mu_4\text{-}SO_4)_3(\mu_3\text{-}OH)_4(\mu_2\text{-}C_2O_4)(\mu_2\text{-}H_2O)(H_2O)_4]\cdot H_2O$ (MCE, $-\Delta S_m^{max}$ = 51.29 J kg^{-1} K^{-1}, the former, $-\Delta S_m^{max}$ = 51.49 J kg^{-1} K^{-1}, the latter).[11] In these two polymers, the light μ_3-hydroxyl anion is beneficial to high magnetic density. However, two complexes mentioned above were obtained by *in situ* reaction, which is difficult to control. Therefore, choosing the low-molecular-weight ligands, such as formate, to modify gadolinium sulfate is a new and feasible strategy for the construction of molecule based magnetic coolers.

Table 2. Comparison of $-\Delta S_m^{max}$ (Larger Than 35.0 J kg^{-1} K^{-1} with $\Delta H \leq 7$ T) among Gd^{III} Containing Complexes Associated with Potential Magnetic Refrigeration

complex	$-\Delta S_m^{max}$ [J kg^{-1} K^{-1}] (ΔH)	$-\Delta S_m^{max}$ [mJ cm^{-3} K^{-1}]
4f		
$[Gd(OH)CO_3]_n$[7c]	66.4 (7 T)	355
$[Gd(O_2CH)_3]_n$[9]	55.9 (7 T)	215.7
$[Gd_4(\mu_4\text{-}SO_4)_3(\mu_3\text{-}OH)_4(\mu_2\text{-}C_2O_4)(\mu_2\text{-}H_2O)(H_2O)_4]\cdot H_2O$[11b]	51.49 (7 T)	190.46
$[Gd_4(SO_4)_4(\mu_3\text{-}OH)_4(H_2O)_4]_n$[11a]	51.29 (7 T)	198.85
3	49.91 (7 T)	189.51
$[Gd(C_2O_4)(H_2O)_3Cl]$[8]	48.0 (7 T)	144
$[Gd6(OH)_8(suc)_5(H_2O)_2]_n\cdot 4nH_2O$[7a]	48.0 (7 T)	144
$[Gd(OAc)_3(H_2O)_{0.5}]_n$[5a]	47.7 (7 T)	106.28
$\{[Gd_6(\mu_6\text{-}O)(\mu_3\text{-}OH)_8(\mu_4\text{-}ClO_4)_4(H_2O)_6](OH)_4\}_n$[16]	46.6 (7 T)	206.81
$[Gd_{24}]$[7b]	46.12 (7 T)	90.03
$[Gd(HCOO)(OAc)_2(H_2O)_2]_n$[17]	45.9 (7 T)	110.02
$[Gd(OAc)_3(MeOH)]_n$[5a]	45.0 (7 T)	96.71
$[Gd(C_4O_4)(C_2O_2)_{0.5}(H_2O)_2]_n$[2b]	44 (7 T)	127.56
$[Gd(C_4O_4)(OH)(H_2O)_4]_n$[1a]	43.8 (7 T)	104.38
$[Gd_{48}]$[18]	43.6 (7 T)	120.7
$[Gd(cit)(H_2O)]_n$[14c]	43.6 (7 T)	115.23
2	43.40 (7 T)	155.76
1	42.88 (7 T)	141.98
$[Gd_2(OH)_2(suc)_2(H_2O)]_n\cdot 2nH_2O$[7a]	42.8 (7 T)	120
$\{[Gd(OAc)_3(H_2O)_2]\}_2\cdot 4H_2O$[5b]	41.6 (7 T)	82.78
$\{[Gd_2(IDA)_3]\cdot 2H_2O\}_n$[4a]	40.6 (7 T)	100.69
$[Gd_{36}]_n$[19]	39.66 (7 T)	91.34
3d−4f		
$\{[Mn(H_2O)_6][MnGd(oda)_3]_2\cdot 6H_2O\}_n$[20]	50.1 (7 T)	114.28
$[Co_{10}Gd_{42}]$[9]	41.26 (7 T)	112.64
$[Ni_{12}Gd_{36}]$[6]	36.3 (7 T)	83.49
$[Cu_3Gd_6]_n$[21]	35.76 (7 T)	90.36
4d−4f		
$[Mo_4Gd_{12}]$[22]	35.3 (7 T)	76.99

CONCLUSION

Three new gadolinium based coordination polymers were obtained by modifying gadolinium sulfate. When the volume ratio of HCOOH and DMSO is increased in the synthesis, the contents of the formate in those complexes are also improved, which enhanced the spin densities and optimized the MCE. The values of the magnetic entropy changes of those complexes are all above 40.0 J kg^{-1} K^{-1}, and complex **3** shows the largest $-\Delta S_m$ of 49.91 J kg^{-1} K^{-1} (189.51 mJ cm^{-3} K^{-1}) for T = 2 K and ΔH = 7 T. The successful synthesis of **1**, **2**, and **3** not only enriches the existing field of molecular magnetic coolers, but also confirms the potential of developing other outstanding complexes with remarkable MCE.

ASSOCIATED CONTENT

Supporting Information

Selected bond lengths, XRPD data, and additional structural figures. The Supporting Information is available free of charge on the ACS Publications website at DOI: 10.1021/acs.inorgchem.5b00214.

AUTHOR INFORMATION

Corresponding Authors

*E-mail: horryzhao@yahoo.com. Phone: (+86) 22-60214259.
*E-mail: fuchenliutj@yahoo.com. Phone: (+86) 22-60214259.

Notes

The authors declare no competing financial interest.

ACKNOWLEDGMENTS

This work was supported by the National Natural of Science Foundation of China (Grants 21471112, 21101114, and 20801041), China Postdoctoral Science Foundation 2013M540029 and 2014T70019, and Beijing City Postdoctoral Science Foundation 2014ZZ-37.

REFERENCES

(1) (a) Biswas, S.; Adhikary, A.; Goswami, S.; Konar, S. *Dalton Trans.* **2013**, *42*, 13331−13334. (b) Evangelisti, M.; Brechin, E.-K. *Dalton Trans.* **2010**, *39*, 4672. (c) Leng, J.-D.; Liu, J.-L.; Tong, M.-L. *Chem. Commun.* **2012**, *48*, 5286. (d) Zheng, Y.-Z.; Pineda, E.-M.; Helliwel, M.; Winpenny, R.-E.-P. *Chem.—Eur. J.* **2012**, *18*, 4161. (e) Nayak, S.; Evangelisti, M.; Powell, A.-K.; Reedijk, J. *Chem.—Eur. J.* **2010**, *16*, 12865. (f) Zheng, Y.-Z.; Zhou, G.-J.; Zheng, Z.-P.; Winpenny, R.-E.-P. *Chem. Soc. Rev.* **2014**, *43*, 1462−1475. (g) Liu, J.-L.; Chen, Y.-C.; Guo, F.-S.; Tong, M.-L. *Coord. Chem. Rev.* **2014**, *281*, 26−49.

DOI: 10.1021/acs.inorgchem.5b00214
Inorg. Chem. 2015, 54, 5249−5256

(2) (a) Zheng, Y.-Z.; Evangelisti, M.; Winpenny, R.-E.-P. *Angew. Chem., Int. Ed.* **2011**, *50*, 3692−3695. (b) Biswas, S.; Jena, H.-S.; Adhikary, A.; Konar, S. *Inorg. Chem.* **2014**, *53* (8), 3926−3928.
(3) (a) Tan, X.-Y.; Chai, P.; Thompson, C.-M.; Shatruk, M. *J. Am. Chem. Soc.* **2013**, *135*, 9553−9557. (b) Roubeau, O.; Lorusso, G.; Teatb, S.-J.; Evangelistia, M. *Dalton Trans.* **2014**, *43*, 11502−11509.
(4) (a) Jia, J.-M.; Liu, S.-J.; Cui, Y.; Han, S.-D.; Hu, T.-L.; Bu, X.-H. *Cryst. Growth Des.* **2013**, *13*, 4631−4634. (b) Sessoli, R. *Angew. Chem., Int. Ed.* **2012**, *51*, 43−45.
(5) (a) Guo, F.-S.; Leng, J.-D.; Liu, J.-L.; Meng, Z.-S.; Tong, M.-L. *Inorg. Chem.* **2012**, *51*, 405−413. (b) Evangelisti, M.; Roubeau, O.; Palacios, E.; Camón, A.; Hooper, T.-N.-E.; Brechin, K.; Alonso, J.-J. *Angew. Chem., Int. Ed.* **2011**, *50*, 6606−6609.
(6) Peng, J.-B.; Zhang, Q.-C.; Kong, X.-J.; Ren, Y.-P.; Long, L.-S.; Huang, R.-B.; Zheng, L.-S.; Zheng, Z.-P. *Angew. Chem., Int. Ed.* **2011**, *50*, 10649−10652.
(7) (a) Chen, Y.-C.; Guo, F.-S.; Zheng, Y.-Z.; Liu, J.-L.; Leng, J.-D.; Tarasenko, R.; Orendáč, M.; Prokleška, J.; Sechovský, V.; Tong, M.-L. *Chem.—Eur. J.* **2013**, *19*, 13504−13510. (b) Chang, L.-X.; Xiong, G.; Wang, L.; Cheng, P.; Zhao, B. *Chem. Commun.* **2013**, *49*, 1055−1057. (c) Chen, Y.-C.; Qin, L.; Meng, Z.-S.; Yang, D.-F.; Wu, C.; Fu, Z.-D.; Zheng, Y.-Z.; Liu, J.-L.; Tarasenko, R.; Orendáč, M.; Prokleška, J.; Sechovskýe, V.; Tong, M.-L. *J. Mater. Chem. A* **2014**, *2*, 9851−9858.
(8) Meng, Y.; Chen, Y.-C.; Zhang, Z.-M.; Lin, Z.-J.; Tong, M.-L. *Inorg. Chem.* **2014**, *53* (17), 9052−9057.
(9) Peng, J.-B.; Zhang, Q.-C.; Kong, X.-J.; Zheng, Y.-Z.; Ren, Y.-P.; Long, L.-S.; Huang, R.-B.; Zheng, L.-S.; Zheng, Z.-P. *J. Am. Chem. Soc.* **2012**, *134*, 3314−3317.
(10) (a) Giauque, W.-F.; MacDougall, D.-P. *Phys. Rev.* **1933**, *43*, 768. (b) Giauque, W.-F.; MacDougall, D.-P. *J. Am. Chem. Soc.* **1935**, *57*, 1175. (c) Hummel, H.-U.; Fixher, E.; Fischer, T.; Joerg, P.; Pezzei, G. *Z. Anorg. Allg. Chem.* **1993**, 619.
(11) (a) Han, S.-D.; Miao, X.-H.; Liu, S.-J.; Bu, X.-H. *Inorg. Chem. Front.* **2014**, *1*, 549−552. (b) Han, S.-D.; Miao, X.-H.; Liu, S.-J.; Bu, X.-H. *Chem.—Asian J.* **2014**, *9*, 3116−3120.
(12) (a) *Crystal Clear and Crystal Structure*; Rigaku/MSC: The Woodlands, TX, 2005. (b) Sheldrick, G. M. *SHELXTL NT Version 5.1. Program for Solution and Refinement of Crystal Structures*; University of Göttingen: Göttingen, Germany, 1997.
(13) (a) Reticular Chemistry Structure Resource (RCSR), http://rcsr.anu.edu.au. (b) Euclidean Patterns in Non-Euclidean Tilings (EPINET), http://epinet.anu.edu.au. (c) Blatov, V. A.; Shevchenko, A. P. *TOPOS 4.0*; Samara State University: Samara, Russia.
(14) (a) Pecharsky, V.-K.; Gschneidner, K.-A. *J. Magn. Magn. Mater.* **1999**, *200*, 44. (b) Zhao, J.-P.; Zhao, R.; Yang, Q.; Hu, B.-W.; Liu, F.-C.; Bu, X.-H. *Dalton Trans.* **2013**, *42*, 14509−14515. (c) Liu, S.-J.; Xie, C.-C.; Jia, J.-M.; Zhao, J.-P.; Han, S.-D.; Cui, Y.; Li, Y.; Bu, X.-H. *Chem.—Asian J.* **2014**, *9*, 1116−1122. (d) Liu, S.-J.; Zhao, J.-P.; Tao, J.; Jia, J.-M.; Han, S.-D.; Li, Y.; Chen, Y.-C.; Bu, X.-H. *Inorg. Chem.* **2013**, *52*, 9163−9165.
(15) (a) Rajeshkumar, T.; Annadata, H. V.; Evangelisti, M.; Langley, S. K.; Chilton, N. F.; Murray, K. S.; Rajaraman, G. *Inorg. Chem.* **2015**, *54*, 1661−1670. (b) Singh, S. K.; Tibrewal, N. K.; Rajaraman, G. *Dalton Trans.* **2011**, *40*, 10897−10906. (c) Rajeshkumar, T.; Singh, S. K.; Rajaraman, G. *Polyhedron* **2013**, *52*, 1299−1305. (d) Cremades, E.; Gómez-Coca, S.; Aravena, D.; Alvarez, S.; Ruiz, E. *J. Am. Chem. Soc.* **2012**, *134*, 10532−10542.
(16) Hou, Y.-L.; Xiong, G.; Shi, P.-F.; Cheng, R.-R.; Cui, J.-Z.; Zhao, B. *Chem. Commun.* **2013**, *49*, 6066.
(17) Lorusso, G.; Palacios, M.-A.; Nichol, G.-S.; Brechin, E.-K.; Roubeau, O.; Evangelisti, M. *Chem. Commun.* **2012**, *48*, 7592.
(18) Guo, F.-S.; Chen, Y.-C.; Mao, L.-L.; Lin, W.-Q.; Leng, J.-D.; Tarasenko, R.; Orendáč, M.; Prokleška, J.; Sechovský, V.; Tong, M.-L. *Chem.—Eur. J.* **2013**, *19*, 14876.
(19) Wu, M.-Y.; Jiang, F.-L.; Kong, X.-J.; Yuan, D.-Q.; Long, L.-S.; Al-Thabaiti, S.-A.; Hong, M.-C. *Chem. Sci.* **2013**, *4*, 3104.
(20) Guo, F.-S.; Chen, Y.-C.; Liu, J.-L.; Leng, J.-D.; Meng, Z.-S.; Vrábel, P.; Orendáč, M.; Tong, M.-L. *Chem. Commun.* **2012**, *48*, 12219.
(21) Bing, Y.-M.; Xu, N.; Shi, W.; Liu, K.; Cheng, P. *Chem.—Asian J.* **2013**, *8*, 1412.
(22) Zheng, Y.; Zhang, Q.-C.; Long, L.-S.; Huang, R.-B.; Müller, A.; Schnack, J.; Zheng, L.-S.; Zheng, Z. *Chem. Commun.* **2013**, *49*, 36.
(23) (a) Gschneidner, K.-A.; Pecharsky, V.-K.; Tsokol, A.-O. *Rep. Prog. Phys.* **2005**, *68*, 1479. (b) Gschneidner, K.-A.; Pecharsky, V.-K. *Annu. Rev. Mater. Sci.* **2000**, *30*, 387. (c) Dan, M.; Behera, J.-N.; Rao, C.-N.-R. *J. Mater. Chem.* **2004**, *14*, 1257−1265.

DOI: 10.1021/acs.inorgchem.5b00214
Inorg. Chem. 2015, 54, 5249−5256